S-MODE Bio-optical Data (V1) Report

Sarah Lang, Melissa Omand, Roger Patrick Kelly

This data report describes the steps taken to quality-control, calibrate bio-optical parameters, and develop biogeochemical proxies from the bio-optical measurements collected during the S-MODE pilot campaign. The S-MODE study area extended about 200 km off the coast of San Francisco (Fig. 1), and the data described in this report were collected between October 22 and November 8, 2021. In this report, we outline our preliminary methods for calibrating bio-optical instruments on the RV *Oceanus*'s underway system, EcoCTD, and 4 Saildrones used during the fall 2021 Pilot Campaign. We also describe our methods for creating optical based proxies of chlorophyll concentrations (Chl; µg/l or mg/$m^{3)}$, particulate organic carbon (POC) molarity (µmol/L), and particulate organic nitrogen (PON) molarity (µmol/L).

Table of contents

Section 1: Data Overview

** Note this list includes only the instruments used for the analysis contained in this report.

RV *Oceanus*:

- Bottle datasets for POC [µmol/L], PON [µmol/L], Chl [mg m^{-3}] and HPLC (pending) were collected from the flow-through system (n = 149) and 2 CTD casts (n = 12).

- Flow-through bio-optical data from a beam attenuation meter (c_p) and chlorophyll-fluorometer (Chl-Fl)
- LI-COR photosynthetically active radiation (PAR) sensor
- EcoCTD tow-yo-ed platform with bio-optical data from a backscatter meter (bb(700)) and chlorophyll-fluorometer (Chl-Fl)

The flow-through (underway) system contained a WETLabs Chlorophyll WETStar Fluorometer from Seabird Scientific, measuring chlorophyll fluorescence (excitation at 460 nm, emission at 695 nm). The flow-through system also had a C-Star Transmissometer from Seabird Scientific, measuring beam transmittance (converted to beam attenuation) with a 25 cm pathlength. The EcoCTD contained an ECO Puck from Seabird Scientific, measuring optical backscatter at 470 nm and 700 nm at a 117˚ scattering angle and chlorophyll-fluorescence.

Saildrone:

- Keel-mounted bio-optical data from a beam attenuation meter (c_p) and chlorophyll-fluorometer (Chl-Fl)

WETLabs BBFL2W ECO Triplets were integrated onto 4 Saildrones, measuring chlorophyll fluorescence (excitation at 470 nm, emission at 695 nm) and optical backscatter at 650 nm at a 117˚ scattering angle. CDOM (colored dissolved organic matter) fluorescence (excitation at 370 nm, emission at 460 nm) was also measured, but excluded from this report.

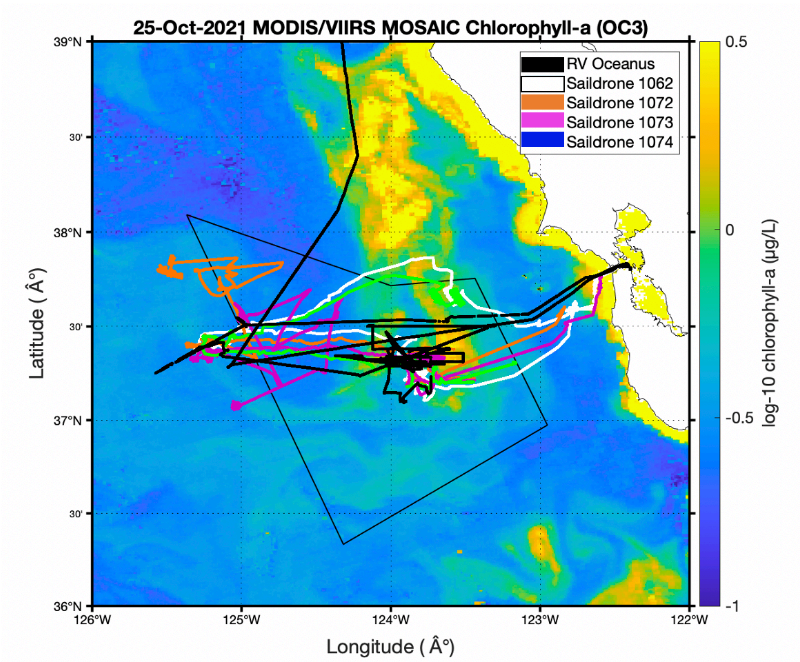

*Fig. 1: MODIS/VIIRS chlorophyll mosaic generated in NASA SeaDAS (*Baith et al., 2001). *Ship tracks (RV Oceanus) and Saildrone tracks overlain.*

Section 2: Ground-truth data: Bottle measurement procedures

2.1 Chlorophyll extractions

Samples for chlorophyll were collected from the R/V Oceanus science seawater system at roughly 30 minute intervals during sampling periods, as well as from 2 CTD casts during the S-MODE cruise. Samples were collected in pre-tared 500 ml LDPE bottles after gently rinsing with sample water 3 times. The samples were then filtered gently through Whatman GF/F filters under low vacuum (5-10 in Hg). After the sample had passed through the filter, the bottle and filter funnels were rinsed 3 times with GF/F filtered seawater. In some cases, titles were subsampled for HPLC pigment analysis using a 10mm diagram arch punch. Sample filters were then placed in 10ml glass cuvette and stored in a dark refrigerator until sampling was complete, at which point 6 ml of 90% acetone / 10% water was added to extract the chlorophyll pigments.

After extracting for 24 hours, the samples were analyzed on a Turner A10 fluorometer. The fluorometer had been calibrated prior to the cruise using a known set of chlorophyll standards and verified during the cruise pre- and post-measurement with a fluorescence cuvette standard. Prior to measurement, samples were vortexed for 5 seconds to remove extracted pigments from the GF/F filter, which was then taken out of the vial. The vial was wiped to remove any residues from the glass and measured for fluorescence in triplicate. Samples that were over the limit were diluted to 3% with 90% acetone and re-analyzed. After completing a batch, phaeopigments were extracted by adding a drop of 10% hydrochloric acid each sample and vortexing it for 5 seconds. After standing for 15 minutes, samples were reanalyzed on the Turner A10.

2.2 Particulate organic carbon and nitrogen

Samples for Particulate Organic Carbon (POC) were collected from the R/V Oceanus science seawater system at predetermined intervals, as well as from 2 CTD casts during the S-MODE cruise. Samples were collected in graduated 4L LDPE bottles after gently rinsing with sample water 3 times. Bottles were filled to 2-4L, based on apparent particle loading estimated from the science seawater system flow-through transmissometer readout. The samples were then filtered gently through pre-combusted Whatman GF/F filters under low vacuum (5-10 in Hg) by inverting the 4L bottle into a filter funnel. In cases where particle loading was substantial, samples that were not completely filtered after ~3 hours were stopped and the remaining sample volume recorded using a 250 ml graduated cylinder. This volume was subtracted from the initial volume to correct for the unfiltered fraction. After the sample had passed through the filter, the bottle and filter funnels were rinsed 3 times with GF/F filtered seawater. Samples were placed in labeled polycarbonate petri dishes and stored frozen until analysis at the University of Rhode Island. Filter funnels and forceps were cleaned with acetone and kim wipes between samples.

Prior to analysis at the University of Rhode Island, samples were dried overnight at 60˚C in a drying oven. They were then subsampled for POC by cutting a visually representative wedge using scissors and forceps cleaned with ethanol. The POC wedge and archive components were then weighed on an analytical balance to determine their relative fraction of the whole filter (15-50% for POC, based on particle loading). The POC subsamples were then exposed to hydrochloric acid fumes in an acid desiccator for 24 hours, while the archive piece was returned to frozen storage. The POC subsamples were then dried again at 60C overnight and packed into 5x9 mm ultra-clean tin capsules and stored in 96-well plates. The POC samples were then analyzed for carbon and nitrogen using a Costech 4010 Elemental Analyzer using aminocaproic acid as the standard.

Section 3: Calibrations

The intensive bottle sampling effort from the R/V Oceanus allowed us to develop proxies for Chl, POC and PON concentration from underway or CTD sensors that are imperfect measurements (i.e. Chl-Fl to Chl concentration) and for sensors that are on different platforms such as the EcoCTD and Saildrone. To establish underway chlorophyll proxies, we fit Chl-Fl and beam attenuation (c_p) to extracted chlorophyll concentrations (from seawater bottle samples taken on a rosette). The underway PAR sensor was used to isolate nighttime fluorescence values to correct for non-photochemical quenching (NPQ). This yielded a Chl-Fl-based chlorophyll proxy and a c_p-based chlorophyll proxy, which agreed well with each other (Fig. 12). POC and PON proxies were developed by fitting underway c_p to bottle samples.

EcoCTD Chl-Fl was intercalibrated with calibrated underway chlorophyll. EcoCTD POC was calibrated by putting the EcoCTD on the rosette and taking optical measurements of c_p and backscatter at 700 nm (bb(700)) at the depth bottle samples were collected. We also used near-surface bb(700) data taken in tow-yo mode and in line bottle samples.

Saildrone 1074 chlorophyll was cross-calibrated with calibrated underway chlorophyll, and Saildrones 1073, 1072, and 1062 were cross-calibrated with Saildrone 1074 (stronger correlations than with underway Chl-Fl). Saildrone POC (bb(650)-based proxy) was cross-calibrated with underway POC as in chlorophyll proxy procedure. EcoCTD and Saildrone PON will be available in V2.

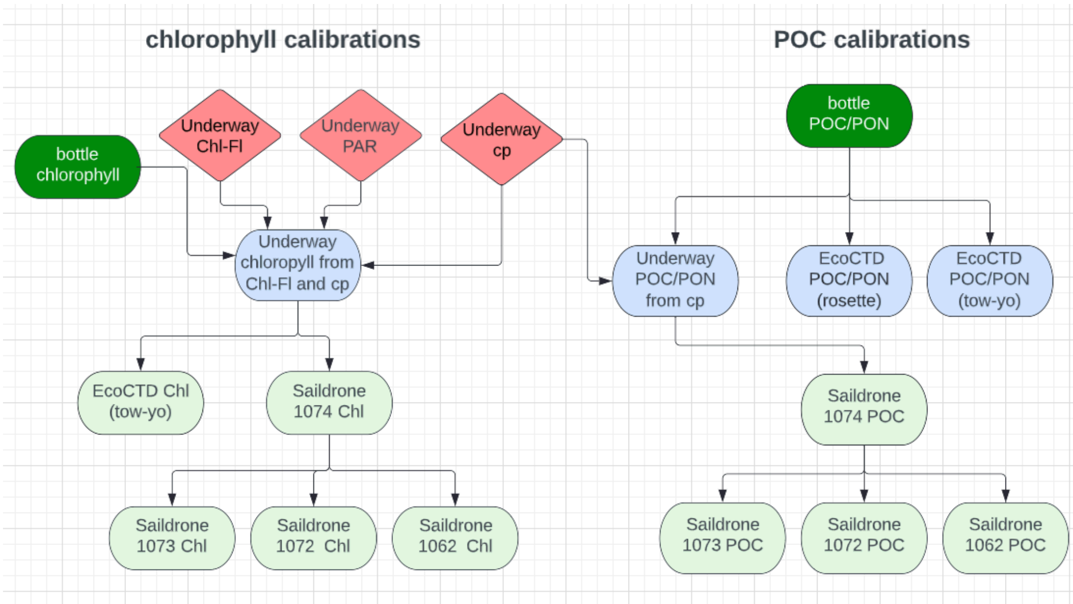

Fig. 2: Order of calibrations. Red denotes optical calibrations used to calibrate underway data. Dark green denotes ground truth measurements (bottle data). Light blue denotes primary optical proxies and green denotes secondary optical proxies (based on intercalibration with primary proxies).

3.1 Optical measurements and initial corrections

3.1.1 Flow-through beam attenuation

Underway data were binned in 1 minute intervals. Factory calibrations, as set by SeaBird Scientific, were applied to raw transmittance values (Eq. 1).

$$Tr = (V_{sig} - V_{dark}) / (V_{ref} - V_{dark}) \quad (1)$$

Where V_{sig} is the raw transmittance measured by the instrument, V_{dark} is the output with the beam blocked (offset), and V_{ref} is output in clean water.

Transmittance was converted to beam attenuation coefficient (c_p, m^{-1}; Eq. 2) with a conversion set by the manufacturer. c_p can also be used as a proxy for chlorophyll (Behrenfeld & Boss 2006).

$$c_p = \frac{-1}{0.25} ln(Tr) \quad (2)$$

where 0.25 is the pathlength of the instrument in meters, and *Tr* is the transmittance (dimensionless).

The instrument experienced significant drift between October 31 and November 5, which was corrected with an empirically-derived linear correction (Eq. 3) based on visual inspection and optimization of the corrected results (Fig. 3).

$$[\text{initial drift correction, } c_p\ (m^{-1})] = [\text{uncorrected } c_p\ (m^{-1})] - \Delta t/10 \quad (3)$$

Where Δt is the time in decimal days between the measurement and the beginning of the drift period. Transmittance values from the beginning of the cruise to November 4 were about 30-40%, corresponding with beam attenuation measurements with a median of 3.9 m^{-1} (value expected in highly turbid waters). Lynn et al. measured beam attenuation coefficients off the coast of Monterey and Pt. Conception in March and April of 1995, with measurements never exceeding 1.6 m^{-1} and dropping to less than 0.4 m^{-1} off coast (2003). These measurements agree well with beam attenuation measured after November 4, indicating a possible partial blockage of the beam for the beginning of the cruise. Therefore, we brought high c_p values from the beginning of the cruise down to the baseline set by the median of c_p (0.659 m^{-1}) measured after November 4 (Fig. 3, green points).

In creating the proxies, we removed a section of erroneous c_p data as indicated by the unnatural shape of the time series (around October 23 – October 25). The section corresponded with the ship going back to port due to mechanical issues.

We also flagged values in Level-1 data (low quality data flagged with "1") outside the likely range of c_p, with variability too large to be corrected (around November 4; Fig. 5). We did not use these data to create proxies.

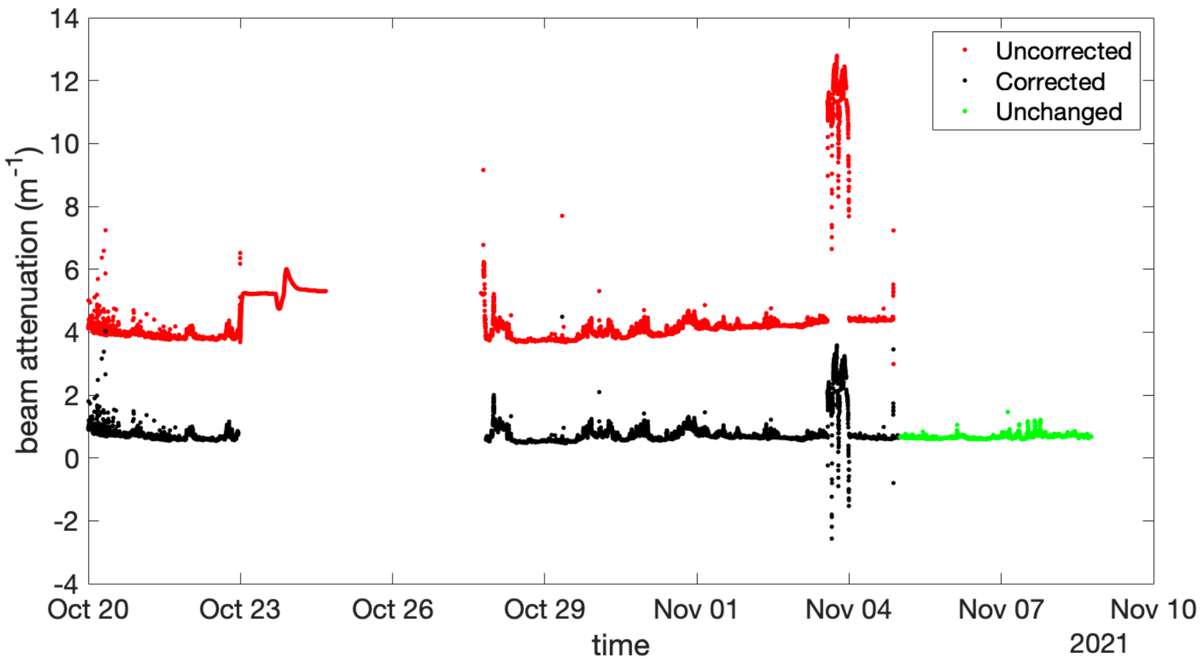

Fig. 3: Time series of corrected (black), uncorrected (red), and unchanged (green) beam attenuation as used in fits for chlorophyll and POC proxies. Data removed where measurement error likely occurred (around Oct 23 – 24). Data around Nov. 4 not used to create proxies.

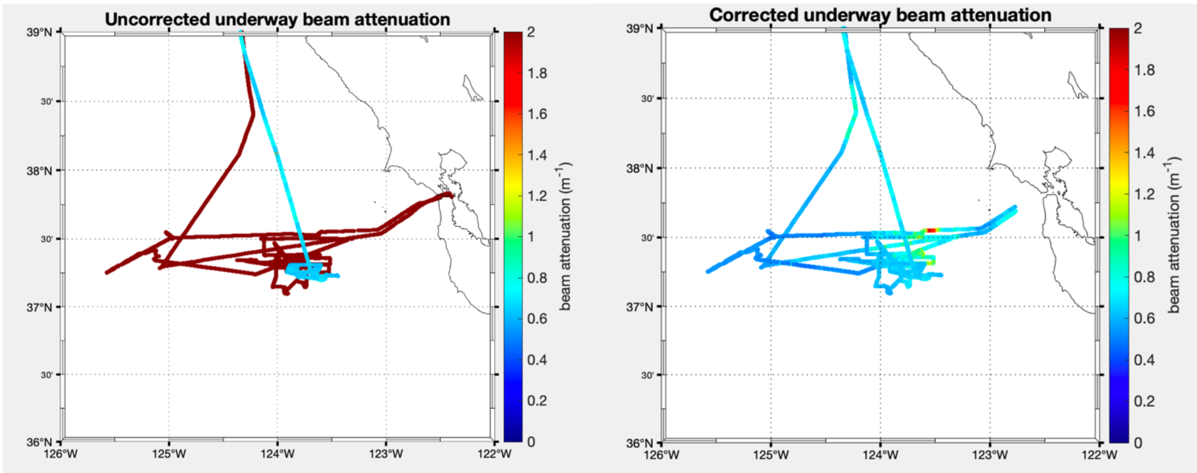

Fig. 4: Uncorrected beam attenuation (left) and corrected beam attenuation (right) off the coast of San Francisco. Uncorrected beam attenuation shows a large difference in values between the beginning of the cruise and the end, most likely due to a partial beam blockage at the beginning (dark red values, left).

3.1.2 Flow-through chlorophyll-fluorescence

Chlorophyll fluorescence from the underway [volts] was binned in 1 minute intervals and left in raw units until calibrated with bottle samples to yield calibrated standard units [µg/L]. Chlorophyll fluorescence from the EcoCTD [counts] was binned in 1 meter vertical bins and converted to (uncalibrated) standard units with factory calibrations provided by WETLabs (Eq. 4).

$$\text{Chl-Fl [µg/L]} = 0.0121 \text{ [µg/L]/count} * (\text{Output} - 49) \text{ counts} \quad (4)$$

where 49 denotes the dark counts. Chlorophyll fluorescence from the Saildrones [counts] were binned in 5 minute intervals and converted to (uncalibrated) standard units as with the EcoCTD (Eq. 5):

$$\text{Chl-Fl [µg/L]} = 0.0071 \text{ [µg/L]/count} * (\text{Output} - 49) \text{ counts} \quad (5)$$

3.1.3 EcoCTD on CTD-Rosette optical backscatter

To calibrate the EcoCTD, 2 calibration casts (October 29, November 5) were taken during the cruise.

Optical backscatter at 700 nm (bb(700)) from the EcoCTD [counts] was converted to standard units ($m^{-1} sr^{-1}$) with factory calibrations provided by WETLabs (Eq. 6):

$$bb(700)\ [m^{-1}sr^{-1}] = 3.186E\text{-}06\ [m^{-1}sr^{-1}]/\text{count} * (\text{Output} - 48) \text{ counts} \quad (6)$$

We applied a 40-point median filter to remove spikes, selecting the filter's order based on the instrument's sampling rate and profiling resolution. Backscatter measurements are at 1 Hz while temperature, salinity, and pressure are at 8 Hz. Therefore, backscatter readings are repeated.

EcoCTD data taken by the cast were significantly higher than tow-yo data - It appears to be best corrected by a linear correction (Eq. 7). This offset, for the same sensor on the same instrument, remains unexplained. Measurements taken from the tow-yo fell within the reasonable range of Saildrone bb(650) (Fig. 9), so cast data was corrected relative to tow-yo data. To develop a correction, we applied factory calibrations and a 40-point median filter to the raw tow-yo data, and compared the closest tow-yo profile in time (18:00 PT) to cast data (18:30 – 19:30 PT). These data had a strong linear relationship (R_{adj}^2 = 96.9%, N = 774; Fig. 5, Eq. 7).

$$[\text{initial cast correction, bb(700) } (m^{-1}\ s^{-1})] = 0.919\ [\text{uncorrected bb(700) } (m^{-1}\ s^{-1})] - 0.00021 \quad (7)$$

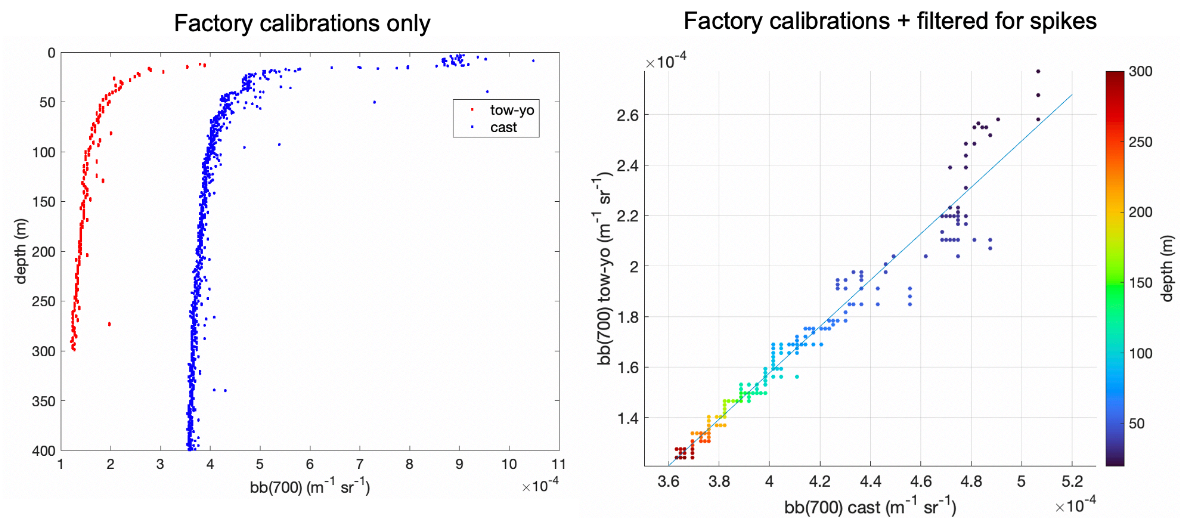

Fig 5: Depth (y-axis) plotted against bb(700) from the tow-yo profile (red) and cast (blue) (left plot). Bb(700) from the cast (y-axis) plotted against bb(700) from the tow-yo (x-axis) (right plot). Points colored by depth. Linear fit in blue.

Upcast and downcast bb(700) agreed well on October 29 (Fig. 6).

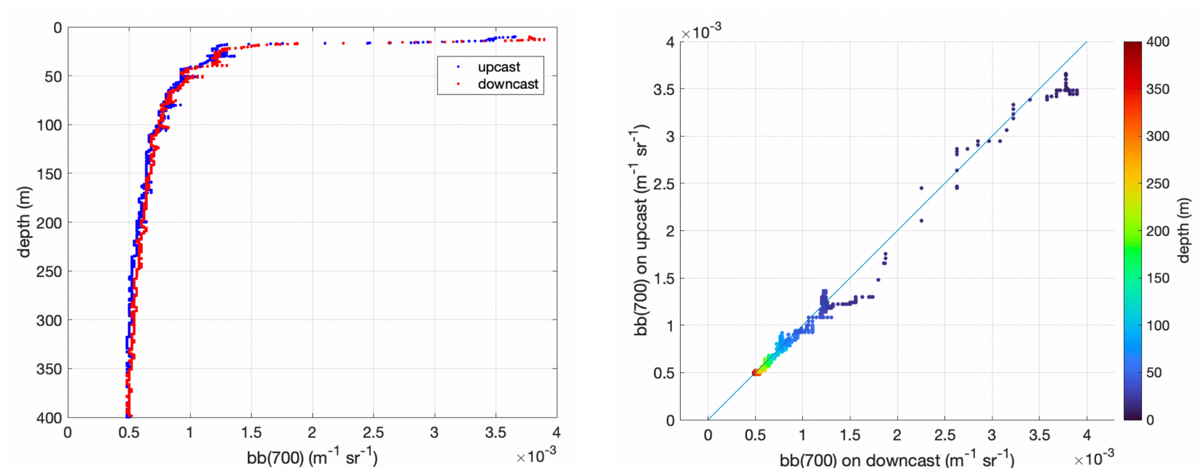

Fig 6: Depth (x-axis) plotted against bb(700) (y-axis) for the upcast (blue) and downcast (red) (left plot). bb(700) on upcast (y-axis) plotted against bb(700) on downcast (x-axis) (right plot). Points colored by depth. 1:1 line in blue.

Backscatter measurements (both bb(700) and bb(443)) from the second cast were unusable due to measurement error. However, bb(700) and c_p from the first cast (10/29) had a strong relationship (R_{adj}^2 = 96.0%; Fig. 9), allowing us to create a bb(700) proxy from c_p to apply to the second cast (Eq. 8). We selected downcast data for the proxy. bb(700) was chosen over bb(443) for POC proxies because Saildrones measure bb(650).

$$[\text{bb(700) proxy } (m^{-1}\ s^{-1})] = (8.33 \times 10^{-3})[c_p\ (m^{-1})] - 1.48 \times 10^{-3} \quad (8)$$

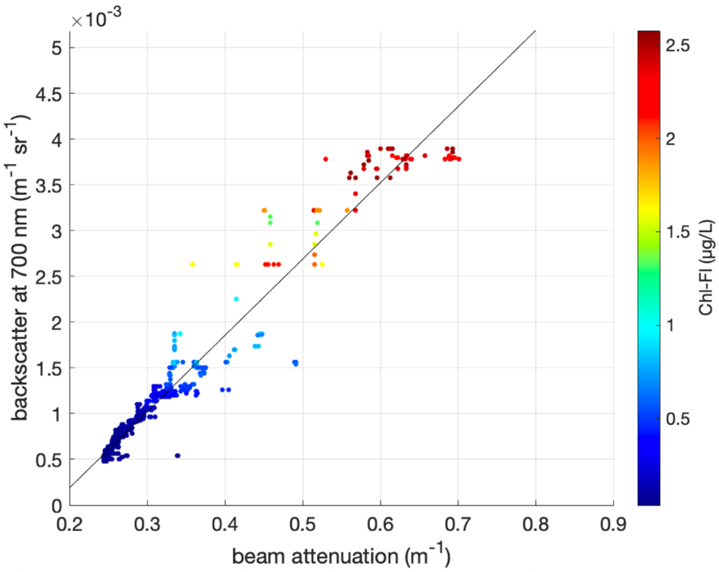

Fig 7: Backscatter at 700 nm (y-axis) plotted against beam attenuation (x-axis) from 10/29 cast. Points colored by chlorophyll-fluorescence (Chl-Fl). Linear fit in black.

Temperature and salinity corrections, as well as a correction for the volume scattering angle, were then applied to all optical backscatter measurements as in Zhang et al. 2009. We used simultaneous *in situ* temperature and conductivity (converted to practical salinity via the Gibbs Seawater (GSW) Oceanographic Toolbox; McDougall & Barker 2011) recorded by the same platform for corrections. Measurements were multiplied by a correction factor of $2\pi\chi$ (χ = 1.076) as in Boss & Pegau 2001.

3.1.4 EcoCTD optical backscatter (tow-yo)

EcoCTD data was binned in 1 meter vertical bins.

Optical backscatter at 700 nm was converted to standard units via factory calibrations in Eq. 5. Optical backscatter at 470 nm (bb(470)) from the EcoCTD [counts] was converted in a similar way (Eq. 9).

$$bb(470)\ [m^{-1}sr^{-1}] = 1.061E\text{-}05\ [m^{-1}sr^{-1}]/count * (Output - 48)\ counts \quad (9)$$

where 48 denotes the dark counts.

Standard corrections (temperature, salinity, volume scattering angle, $2\pi\chi$ factor) were applied to tow-yo data as with cast data.

3.1.5 Saildrone optical backscatter

Saildrone data was binned in 5 minute intervals. Standard corrections (temperature, salinity, volume scattering angle, $2\pi\chi$ factor) were applied. Saildrone 1074, 1073, and 1062 data fell within range of EcoCTD data (Fig. 8). A +0.0007 $m^{-1}sr^{-1}$ offset was applied to bb(700) from Saildrone 1072 (chosen based on visual inspection). A 10 point median filter was then applied to data remove spikes.

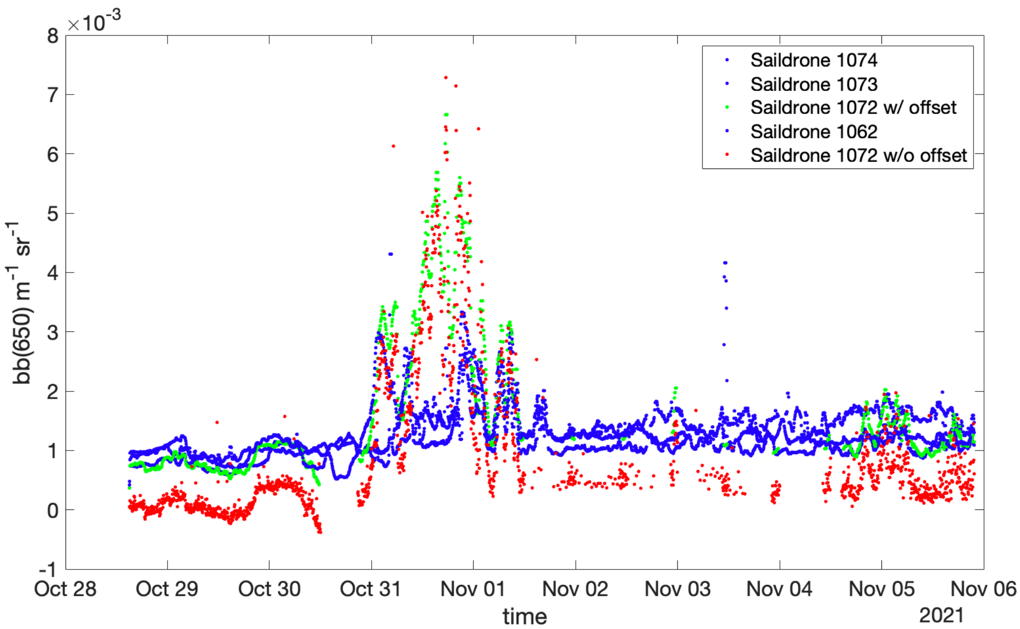

Fig 8: Saildrone bb(650) (y-axis) plotted against time (x-axis) for period EcoCTD was deployed. Points colored by Saildrone. Saildrone 1072 without offset in red and with offset applied in green.

Although Saildrone bb(650) (< 4 km away from ship) fell within range of EcoCTD bb(700), measurements are not correlated (Fig. 9). Relatively few (n = 11, 7, 6, and 8 for 1074, 1073, 1072, and 1062) Saildrone match-ups occurred close to the ship (<2.5 km distance) while the EcoCTD was deployed, and the variability during these match-ups was fairly small (1 to 2 $x10^{-3}$ $m^{-1}sr^{-1}$) which likely explains the lack of correlation. In general, however, they are both in the same range, so we determined that no further correction was required.

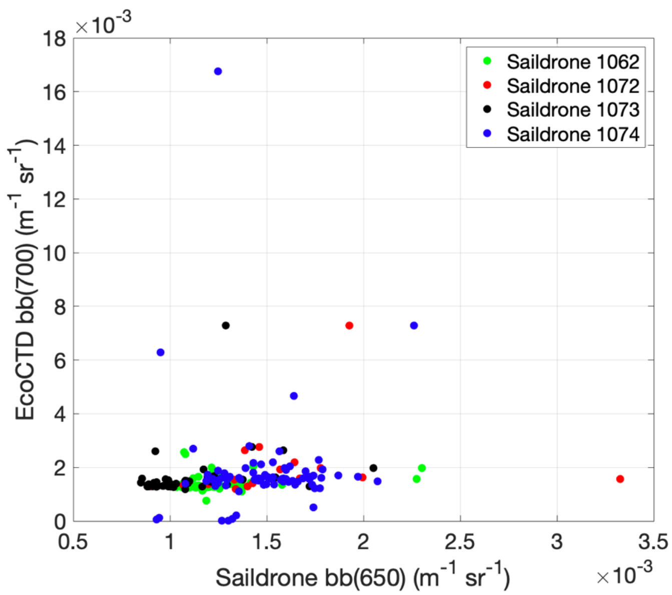

Fig 9: EcoCTD bb(700) (y-axis) plotted against Saildrone bb(650) for Saildrones 1074, 1073, 1072, and 1062. Points colored by Saildrone.

3.4 Primary optical proxies (directly from bottle measurements)

3.2.1 Chlorophyll-a (Chl) proxies from flow-through chlorophyll-fluorescence and beam attenuation

Nighttime fluorescence values from the underway were isolated by using a PAR threshold of 0.31 volts (selected based on an examination of a $\log_{10}$(PAR) time series). Daytime fluorescence values were excluded to avoid the effects of non-photochemical quenching (NPQ, Fig. 10).

We fit a line between chlorophyll concentrations (from extracted chlorophyll fluorescence) from seawater samples and nighttime fluorescence measured in-line, minimizing the mean square error. This fit yielded an empirical formula for chlorophyll-fluorescence (volts) to calibrated chlorophyll concentrations (µg/L) (Eq. 10, Fig. 10).

$$[\text{calibrated chlorophyll } (\mu g/L)] = 3.96*[\text{Chl-Fl (volts)}] - 0.778 \qquad (10)$$

This calibration brought low chl values near 10/23-10/24 slightly below 0, so we set these equal to 0. All negative deviations from 0 (average deviation = -0.15 ± 0.042 µmol/L, maximum deviation = - 0.25 µmol/L) were less than the RMSE of this fit (RMSE = 0.57 µmol/L).

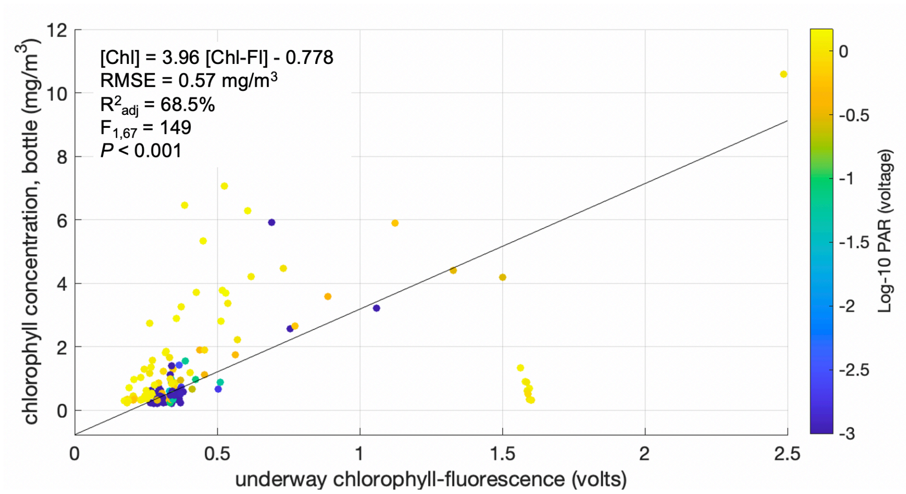

Fig. 10: Chlorophyll concentrations from bottle samples (y-axis) plotted against underway Chl-Fl (x-axis). Points are colored by log-10 PAR. Daytime (yellow and orange) values were excluded from the fit to avoid the effect of non-photochemical quenching.

We found that a power law (R_{adj}^2 = 72.6%) between underway beam attenuation (c_p) and bottle chlorophyll (blue line; Eq. 11, Fig. 11) captured smaller values better than a simple linear regression (R_{adj}^2 = 74.6%; red line; Fig. 11). An outlier (denoted by x in Fig. 11) was left out of the fit due to its significant weight on the fit.

$$[\text{calibrated chlorophyll } (\mu g/L)] = 3.46\ [c_p\ (m^{-1})]^{3.40} \qquad (11)$$

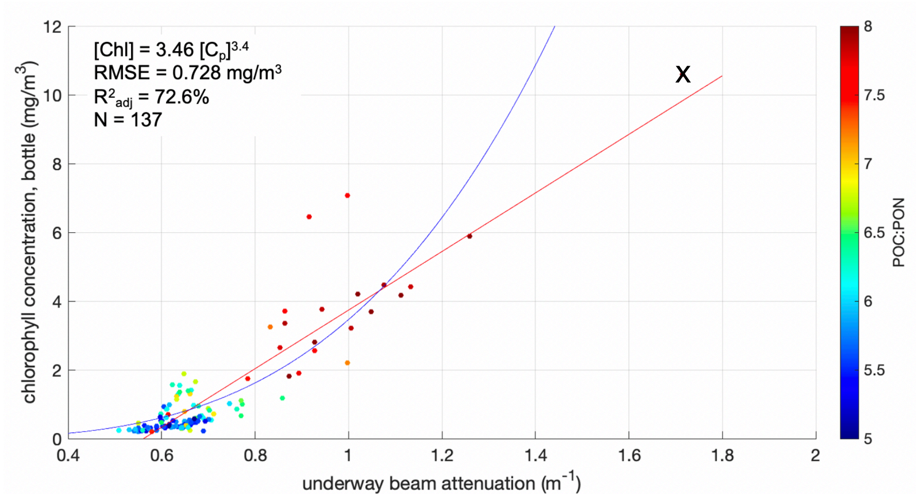

Fig. 11: Chlorophyll concentrations from bottle samples (y-axis) plotted against underway beam attenuation (x-axis). A power law fit (blue, provided statistics) captured lower chlorophyll values better than a simple linear regression (red). Outlier left out of regression denoted by x. Points colored by POC:PON ratio.

The calibrated fluorescence-based proxy (Chl-Fl, μg/L) and calibrated c_p - based proxy (Chl- c_p; μg/L) agree well with each other and extracted chlorophyll samples (Fig. 12a). However, there are departures between Chl-Fl and c_p at low chlorophyll values at the end of the cruise (Fig. 12b). Spatial differences were also observed between the two proxies (Fig. 12c). This will be further investigated for version 2. Based on the shift in the POC:PON ration, it is possible that the high Chl points causing the curve upward may be a different population with a different Chl:carbon ratio. In that case, we may move to linearly fit these two populations separately. **The use of the Chl-Fl proxy is recommended at this time**. In the next version of the data, we will also investigate a different approach to NPQ correction.

a)

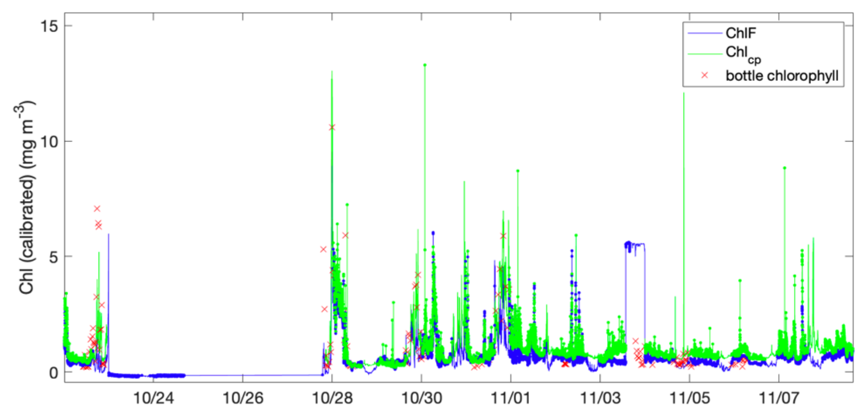

b)

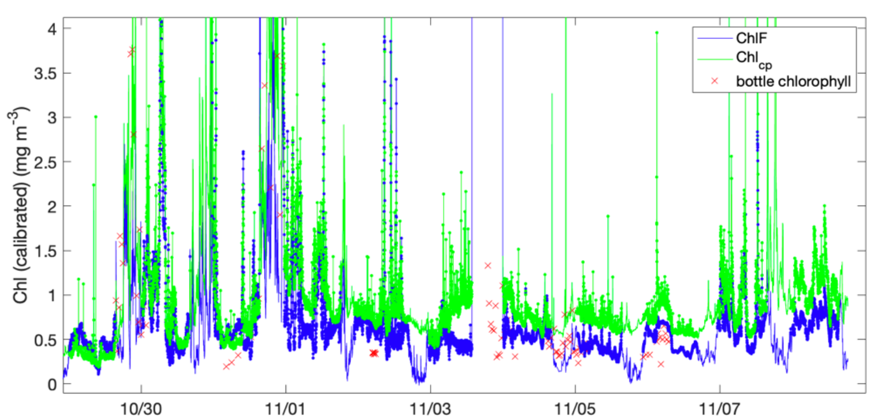

c)

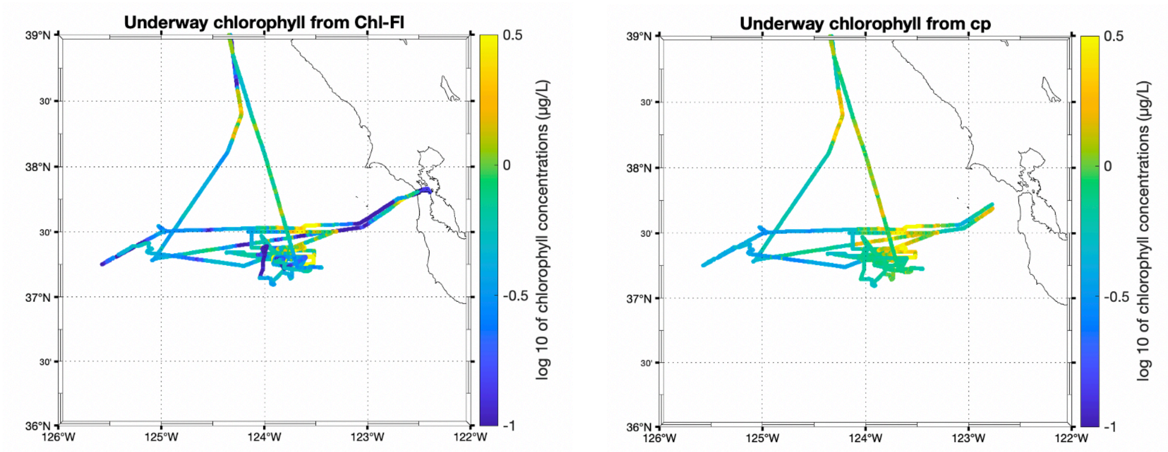

Fig. 12: Fluorescence-based chlorophyll proxy (blue, ChlF) and beam attenuation-based chlorophyll proxy (green, Chl-C_p) plotted against time from October 22 to November 8 (a). Extracted chlorophyll values denoted by red x. In the time series of October 30 to November 8, differences between the two proxies at low chlorophyll concentrations are discernible (b). Maps of Chl-Fl based chlorophyll proxy (left, c) and cp-based chlorophyll proxy (right, c). Points colored by the log-10 of chlorophyll concentrations (µg/L).

3.4.2 Particulate organic carbon (POC) and nitrogen (PON) proxies from flow-through beam attenuation (c_p)

Underway beam attenuation (m^{-1}; Fig. 13) was a strong predictor for POC (µmol/L; R_{adj}^2 = 92.1%, Fig. 13 left, Eq. 12) and PON (µmol/L; R_{adj}^2 = 90.2%, Fig. 13 right, Eq. 13).

$$[\text{calibrated POC } (\mu\text{mol/L})] = 42.5\ [c_p\ (m^{-1})]^{3.03} \qquad (12)$$
$$[\text{calibrated PON } (\mu\text{mol/L})] = 5.53\ [c_p\ (m^{-1})]^{2.74} \qquad (13)$$

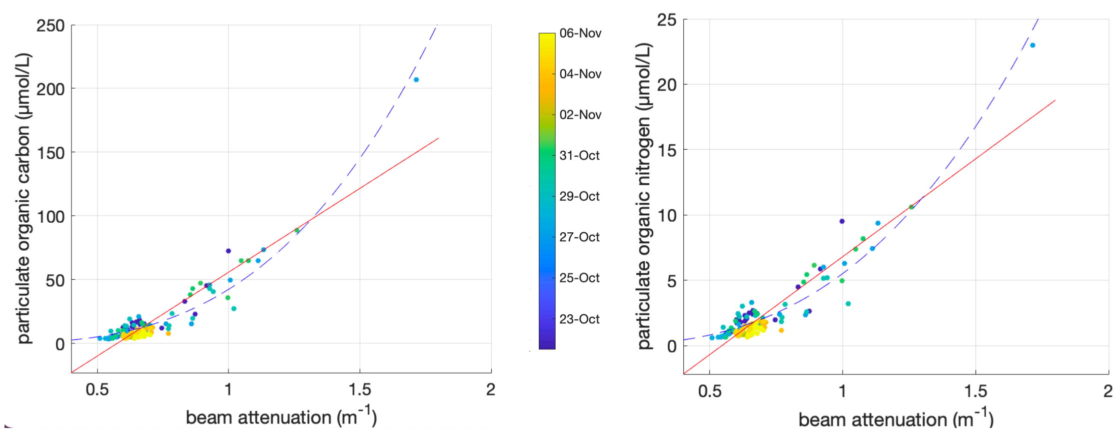

Fig. 13: Particulate organic carbon (POC, y-axis, left) and particulate organic nitrogen (PON, y-axis, right) plotted against beam attenuation (c_p; x-axis). Points colored by day. Power fit (blue dashed line, graph statistics) was a better fit than a linear regression (red solid line).

a)

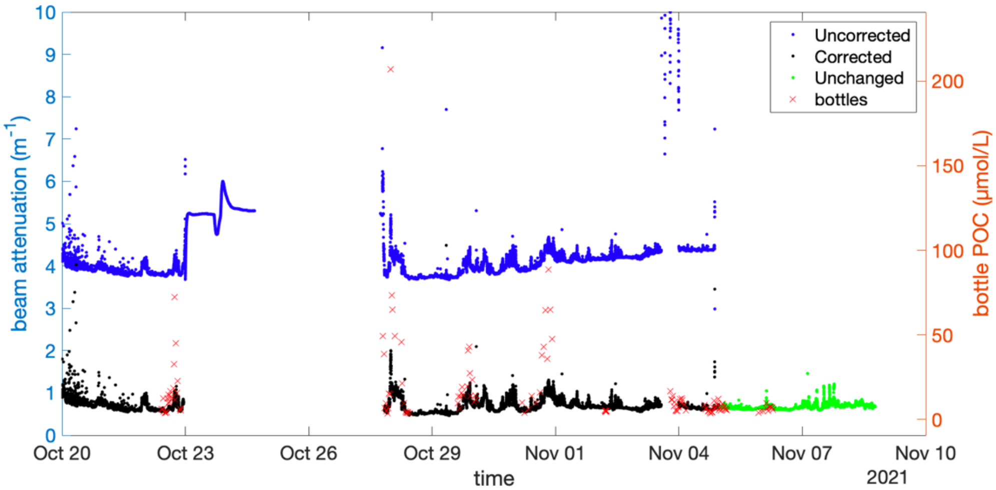

b)

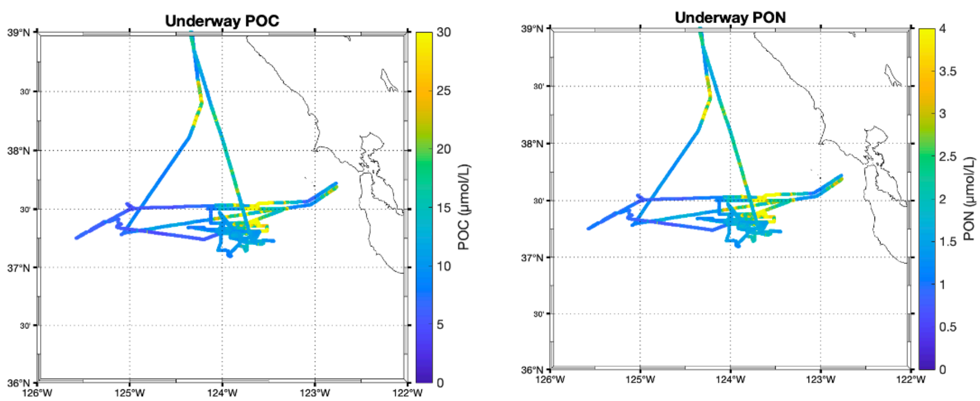

Fig 14: Uncorrected (blue), corrected (black), and unchanged (green) beam attenuation (left y-axis) plotted as a function of time (x-axis) (a). Particulate organic carbon molarity (right y-axis), denoted by red x's, plotted as a function of time (a). POC and PON maps (b), with tracks colored by molarity (µmol/L).

<u>3.4.3 Particulate organic carbon (POC) and nitrogen (PON) proxies from EcoCTD bb(700) on CTD-Rosette and near-surface EcoCTD bb(700) (tow-yo)</u>

A line was fit through all cast data and near-surface tow-yo data to create an EcoCTD POC proxy (R_{adj}^2 = 84.9%, $F_{1,69}$ = 394, $P < 0.001$; Fig. 15, Eq. 14). Removed outlier in red (> 2 standard deviations away from fit; standard deviation of fit = 10.7 µmol/L, observation fell 23.5 µmol away from fit).

$$[\text{POC } (\mu\text{mol/L})] = 8142\ [\text{bb}(700)\ (\text{m}^{-1}\text{sr}^{-1})] - 4.85 \qquad (14)$$

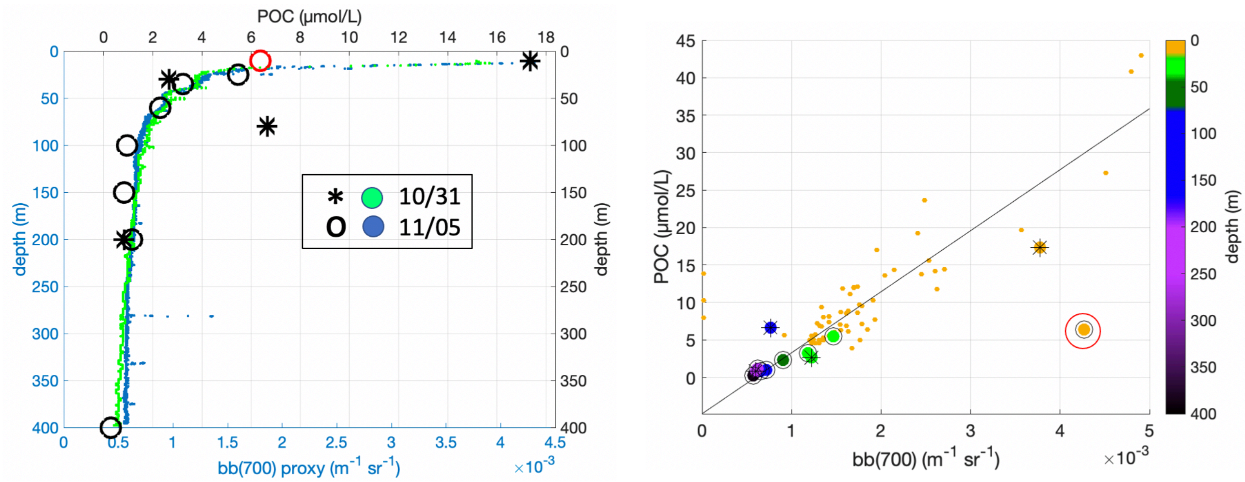

*Fig. 15: Left plot: Depth (y-axis) plotted against POC (top x-axis, denoted by discrete data points) and bb(700) (bottom x-axis, in blue and green). POC bottle data from 10/31 denoted by * and bb(700) data from ECO Puck in green. POC bottle data from 11/05 denoted by o and bb(700) data from ECO Puck in blue. Outlier in red. Right plot: Particulate organic carbon (y-axis) plotted against bb(700) (x-axis). Points colored by depth of measurement. * denotes measurements from the first calibration cast on October 31, and o denoted measurements from the second calibration cast on November 5. Outlier excluded from fit circled in red. Near-surface bb(700) from tow-yo data plotted in small orange points.*

We followed the same procedure to create an EcoCTD PON proxy (R_{adj}^2 = 81.5%, $F_{1,69}$ = 308, $P < 0.001$; Fig. 16, Eq. 15). We removed the same outlier as above (red circle; Fig. 16).

$$[\text{PON } (\mu\text{mol/L})] = 994.3\ [\text{bb}(700)\ (\text{m}^{-1}\text{sr}^{-1})] - 3.09 \qquad (15)$$

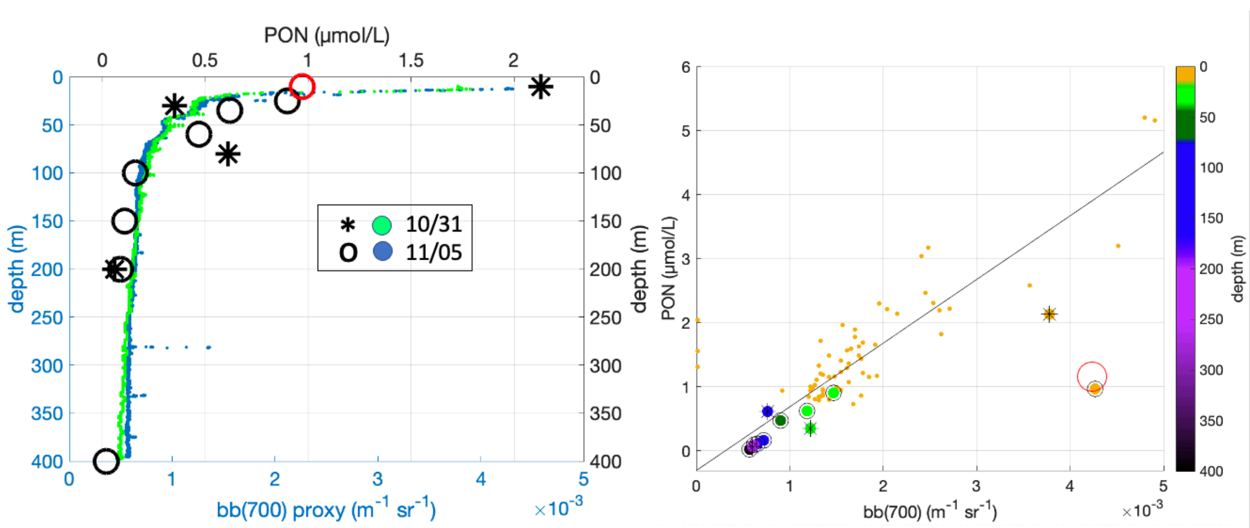

Fig. 16: Particulate organic nitrogen (PON) data plotted as POC data in Fig. 15.

We applied these proxies to binned (1 meter vertical bins) Level-3 EcoCTD data (Fig. 17, 18).

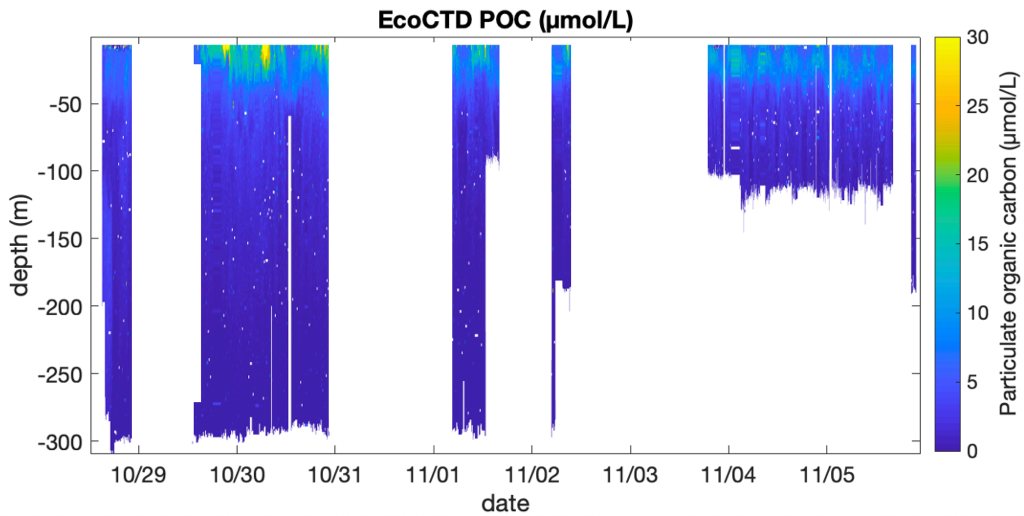

Fig. 17: Depth (y-axis) plotted against time (x-axis) and colored by POC (μmol/L).

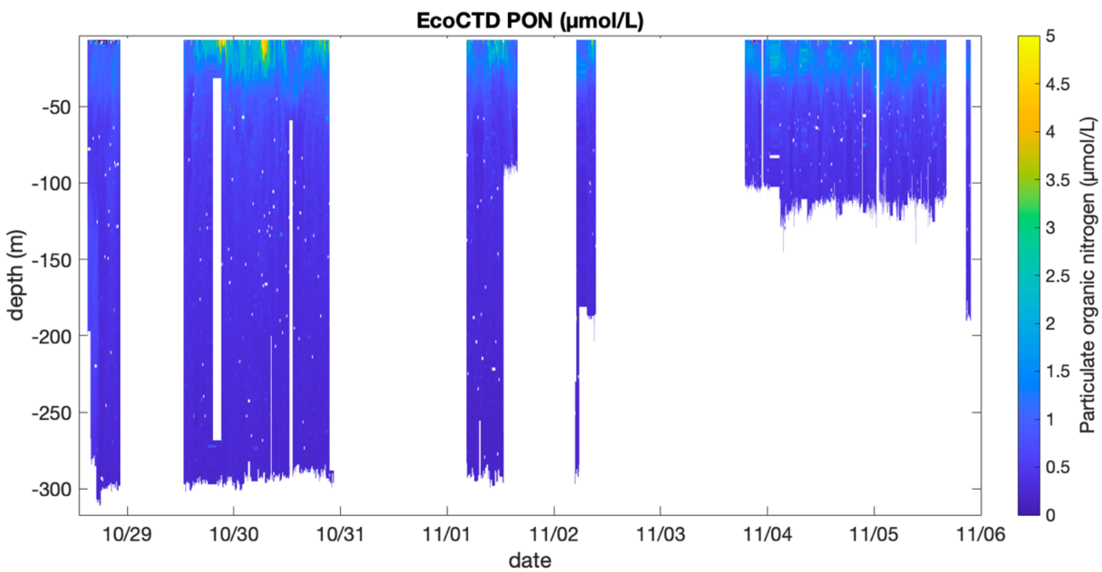

Fig. 18: Depth (y-axis) plotted against time (x-axis) and colored by PON (μmol/L).

3.3 Secondary optical proxies (developed based on intercalibration with primary proxy)

3.3.1 EcoCTD Chl (calibrated from flow-through Chl)

Underway and near-surface (at ~7 meters depth) EcoCTD Chl-Fl measurements were matched up by closest time (< 1 minute apart). Negative EcoCTD Chl-Fl data were removed. Near-surface EcoCTD chlorophyll-fluorescence agreed well with underway chlorophyll-fluorescence (Fig. 19, Fig. 20) except for two times along the time series (denoted by dashed boxes in Fig. 19). The first mismatch could be due to the offset in measurement depth, while the second mismatch is most likely due to underway measurement error. These points were removed from the fit.

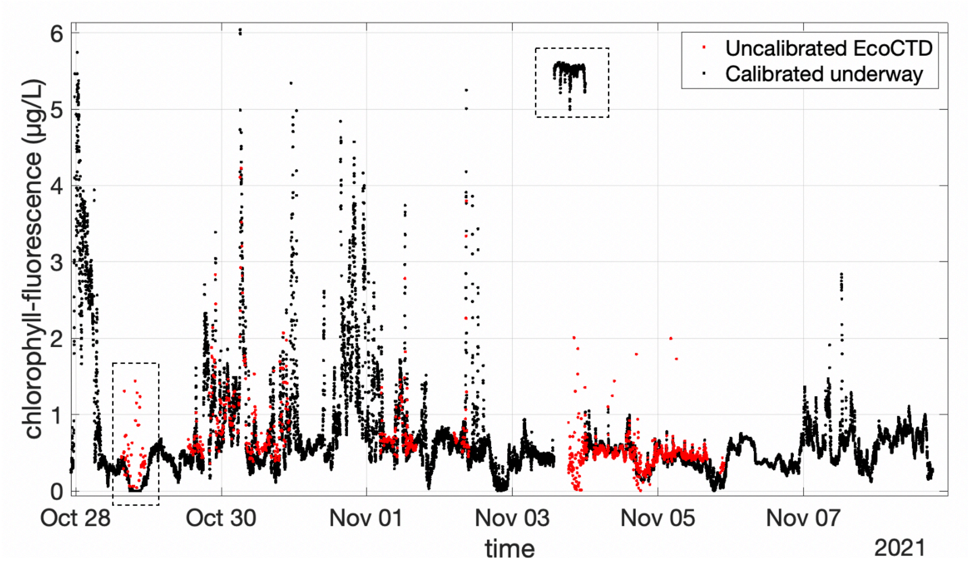

Fig. 19: Near-surface EcoCTD (red) and underway (black) chlorophyll fluorescence (y-axis) plotted against time (x-axis). Times where poor agreement between the instruments occurred outlined in black dashed box.

A linear fit between underway Chl-Fl and near-surface EcoCTD Chl-Fl was significant (R_{adj}^2 = 85.7%, $F_{1,2393}$ = 1.43 x 10^4, $P < 0.001$; Fig. 20), and close to a 1:1 line (Eq. 16).

$$[\text{Chl } \mu\text{g/L}] = 1.02\ [\text{uncalibrated Chl-Fl } (\mu\text{g/L})] - 0.058 \qquad (16)$$

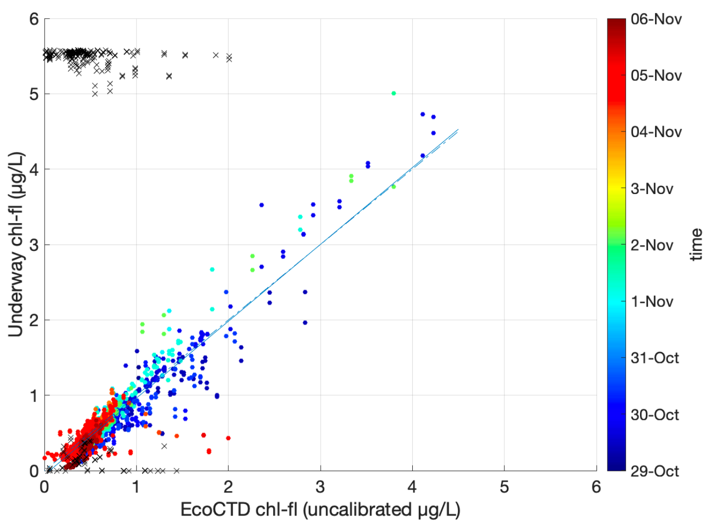

Fig 20: Underway Chl-Fl (y-axis) plotted against near-surface EcoCTD Chl-Fl (x-axis). Points colored by date. Linear fit (Eq. 8) in blue, 1:1 line dashed. Linear fit falls close to 1:1 line.

After applying the chlorophyll corrections to binned (1 meter vertical bins) Level-3 EcoCTD data, negative values were removed. Near zero negative values (~ -0.1) were brought to zero.

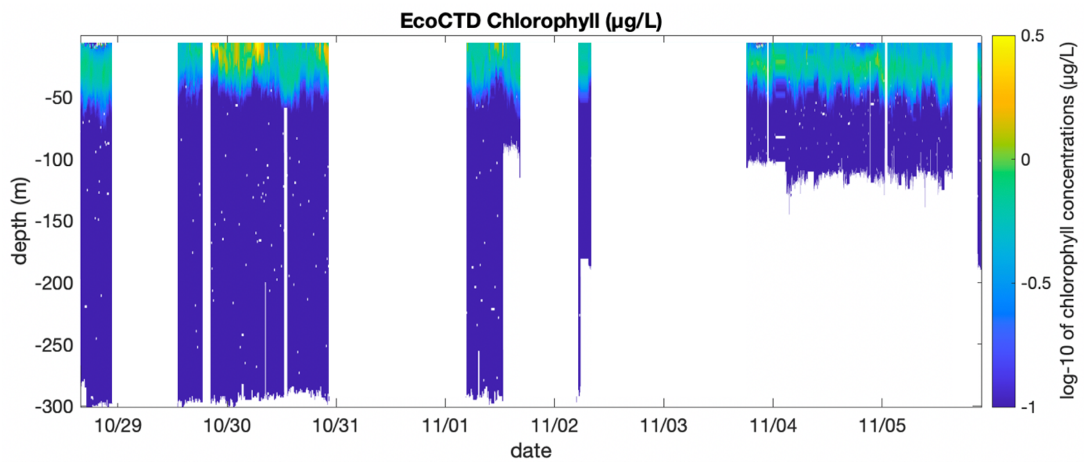

Fig 21: Depth (y-axis) plotted against time (x-axis) and colored by EcoCTD chlorophyll-concentrations (µg/L).

<u>3.3.2 Saildrone Chl-Fl</u>

We matched underway data and Saildrone 1074 data by closest time (<1 minute apart) and selected a distance threshold with enough data points and the best fit. There was a positive relationship between distance and difference in measured values for distances less than 5 km between the ship and the reference Saildrone 1074 (Fig. 20). Additionally, there appears to be a high chlorophyll region (points in red, Fig. 20 left) captured by the underway during a time the ship was 2.3 – 25 km away from the Saildrone. We chose a distance threshold of < 2 km between the ship and reference Saildrone 1074. Saildrone 1073 was calibrated with all measurements within 1.5 km of Saildrone 1074, Saildrone 1072 within 1.5 km, and Saildrone 1062 within 2.4 km.

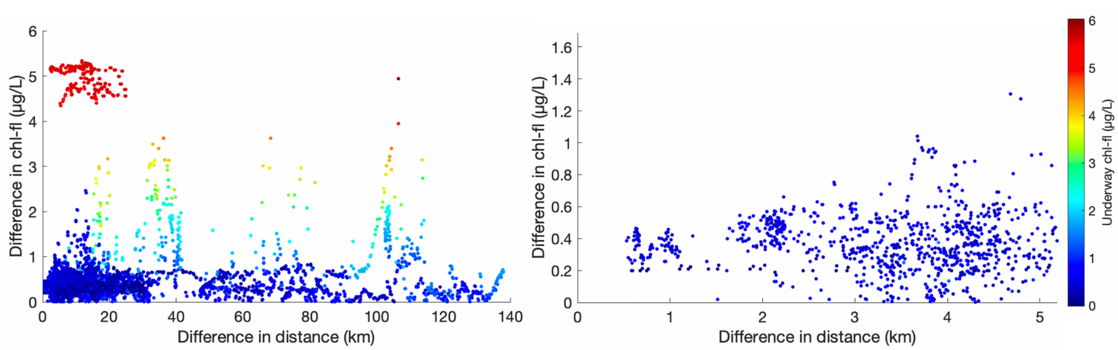

Fig. 22: Difference between underway fluorescence and Saildrone 1074 fluorescence plotted against distance between ship and Saildrone-1074 (left). Under 5 kilometers (right), difference and distance apart have a positive relationship.

<u>Model-fitting procedure</u>

We followed the same model fitting procedure for underway-Saildrone and Saildrone-Saildrone intercalibrations. First, we fit a line between chlorophyll-fluorescence measured by the reference instrument (x, eg. calibrated underway) and chlorophyll-fluorescence measured by the instrument being calibrated (y, eg. Saildrone 1074). We expected chlorophyll concentrations to equal 0 µg/L at a fluorescence of 0 µg/L, so we subtracted the offset (b_{off} ; intercept of fit) from y.

$$y = m_1 x + b_{off} \rightarrow y - b_{off} = m_1 x \qquad (17)$$

where m_1 is the slope and b_{off} is the intercept of this fit. In the cases where the linear fit yielded a slope that varied significantly from 1, we fit a line to low chlorophyll values (stronger relationships between x and y) to calculate the offset (b_{off}).

Chlorophyll was log-normally distributed, so we plotted log(y- b_{off}) against log(x) and fit a line between the two values (Eq. 18).

$$\log(y - b_{off}) = m_{log}\log(x) + b_{log} \rightarrow y = 10^{b_{log}} x^{m_{log}} + b_{off} \qquad (18)$$

We expect a linear relationship between log(y- b_{off}) and log(x)), so we forced the slope of the log-log plot to 1. Contrary to the simple linear fit, the log models avoid giving disproportionate weights to higher values and accounts for instrument error that may cause non-zero fluorescence values at 0 µg/L of chlorophyll. The final model follows the form of Eq. 19:

$$y = 10^{b_{log}} x + b_{off} \qquad (19)$$

Results

Underway Chl-Fl and Saildrone 1074 Chl-Fl were highly correlated (linear fit: R^2_{adj} = 90.7%, $F_{1,361}$ = 1310.5, $P <$ 0.001). The linear fit was close to the log fit (Fig. 23, left).

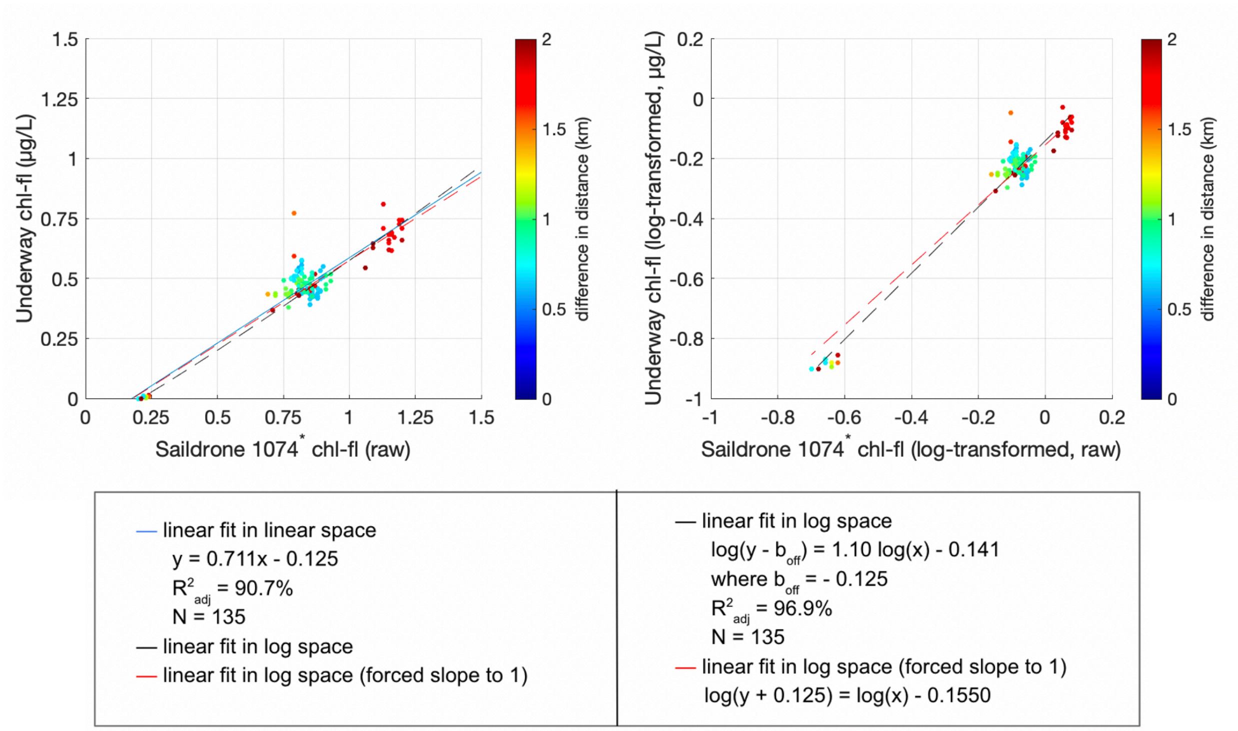

Fig. 23: Saildrone 1074 Chl-Fl (x-axis) plotted against calibrated underway Chl-Fl (y-axis) in linear space (left) and in log-log space (right). Data points colored by distance between ship and Saildrone. In the log-log plot, an offset has been subtracted from the Saildrone 1074 measurements as in Eq. 17. Fit in linear space denoted by solid blue line and linear fits in log space (black: slope not forced; red: slope forced to 1) denoted by dotted lines. Equations and metrics for each fit given.

The fits between Saildrone 1074 chlorophyll and Saildrone 1073 Chl-Fl ($R_{adj}^2 = 71.1\%$, $F_{1,69} = 173$, $P < 0.001$; Fig. 24), Saildrone 1072 Chl-Fl ($R_{adj}^2 = 43.6\%$, $F_{1,114} = 89.8$, $P < 0.001$; Fig. 24) and Saildrone 1062 Chl-Fl ($R_{adj}^2 = 55.4\%$, $F_{1,35} = 45.7$, $P < 0.001$; Fig. 24) were significant.

Saildrone 1073 chl calibration

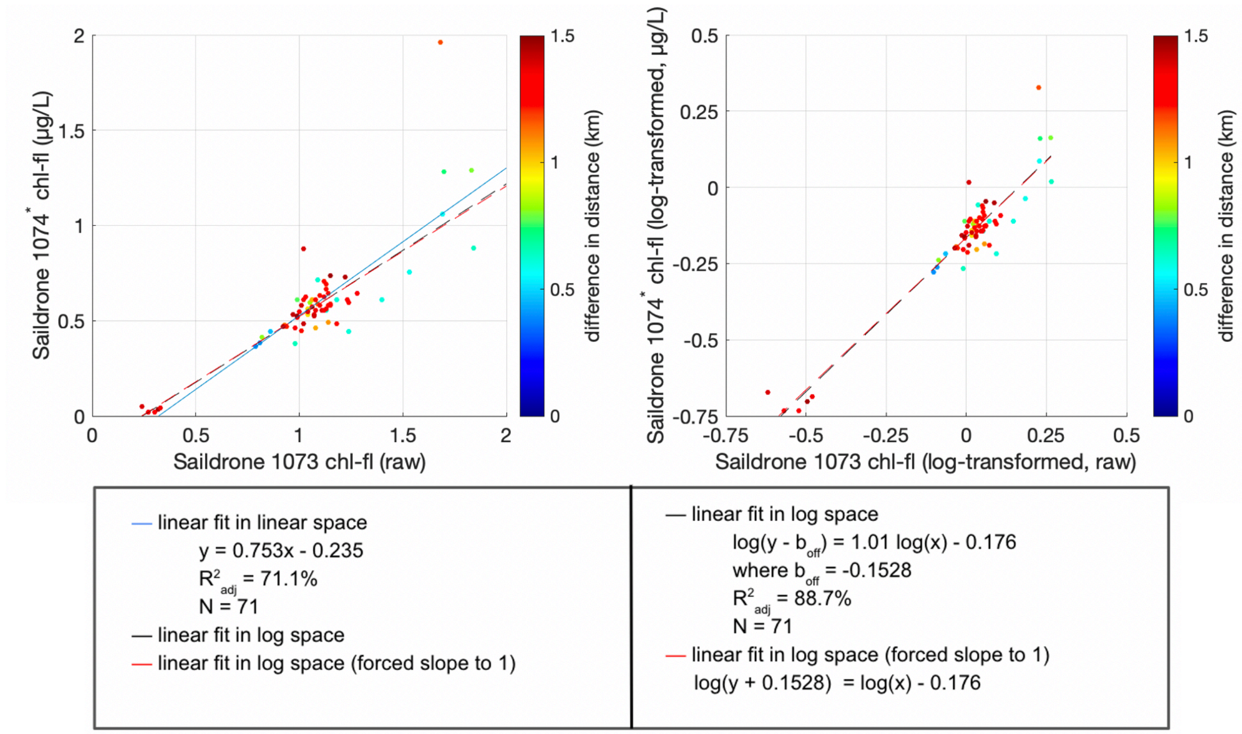

Saildrone 1072 chl calibration

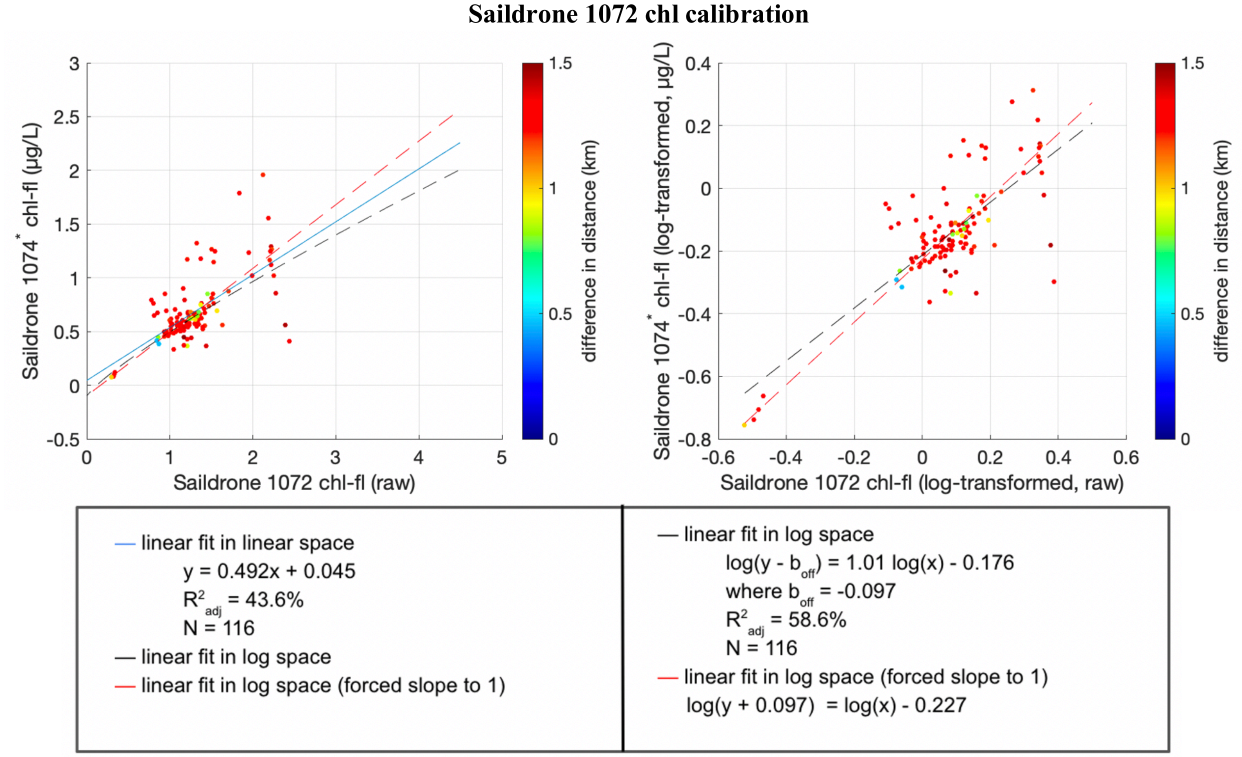

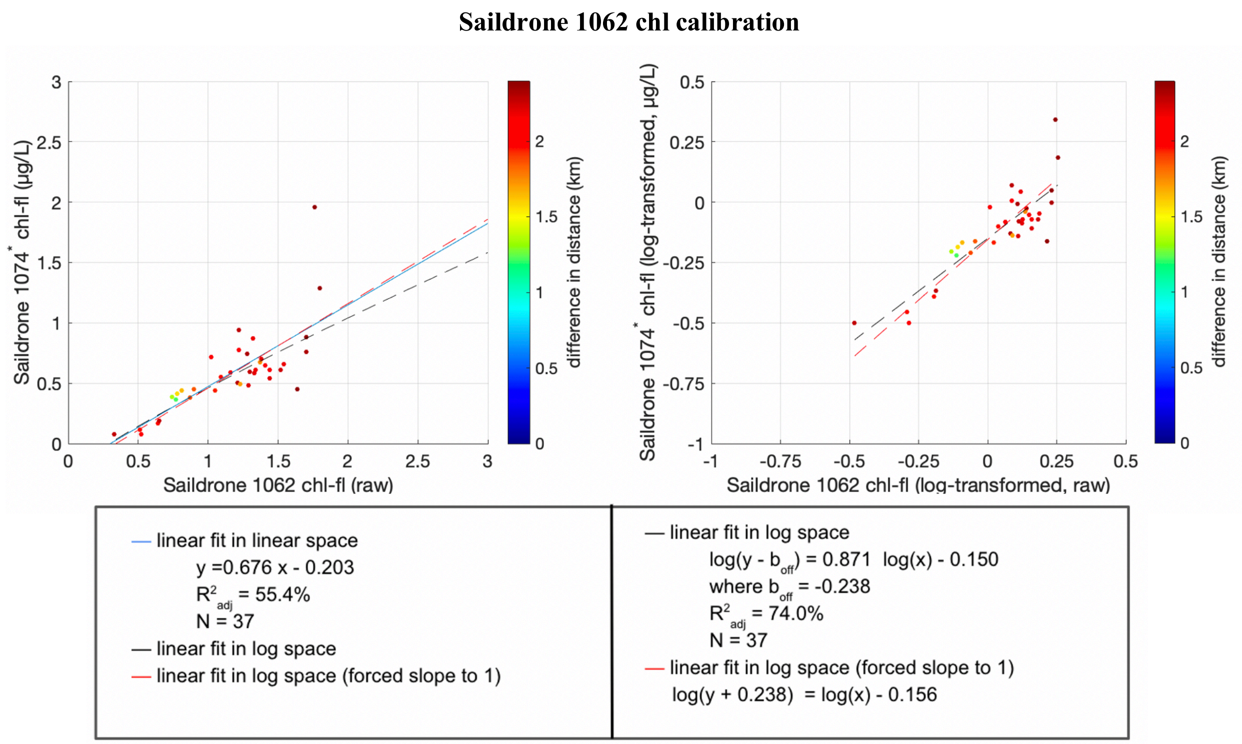

Fig. 24: Saildrone 1074 Chl-Fl (y-axis) plotted against Saildrone 1073 Chl-Fl (x-axis) in linear space (left) and in log-log space (right). Data points colored by distance between Saildrones. Fits as in Fig. 23.

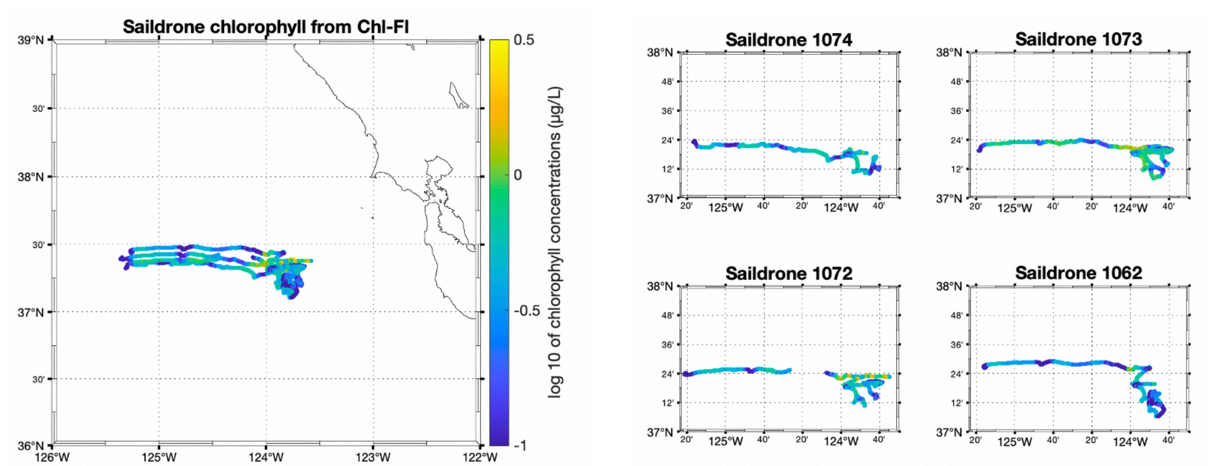

Fig. 25: Saildrone tracks colored by log-10 chlorophyll.

After applying the corrections, some Saildrone 1062 chlorophyll values dip slightly below 0 (minimum ~ -0.09 μg/L). However, all negative values were less than the RMSE of the fit (0.22 μg/L), so these values were set equal to 0.

See Section 4 for equations.

<u>3.3.4 Saildrone POC</u>

Saildrone bb(650) and underway POC were matched up as in Saildrone Chl procedure above. We chose a distance threshold of < 1.5 km between the ship and reference Saildrone 1074. Saildrone 1073 was calibrated with all measurements within 2 km of Saildrone 1074, Saildrone 1072 within 1.5 km, and Saildrone 1062 within 2.4 km.

The fits between Saildrone 1074 POC and Saildrone 1073 bb(650) (R_{adj}^2 = 64.7%, $F_{1,346}$ = 637, P < 0.001; Fig. 26), Saildrone 1072 bb(650) (R_{adj}^2 = 86.4%, $F_{1,92}$ = 590, P < 0.001; Fig. 26) and Saildrone 1062 bb(650) (R_{adj}^2 = 32.3%, $F_{1,35}$ = 18.2, P < 0.001; Fig. 26) were significant.

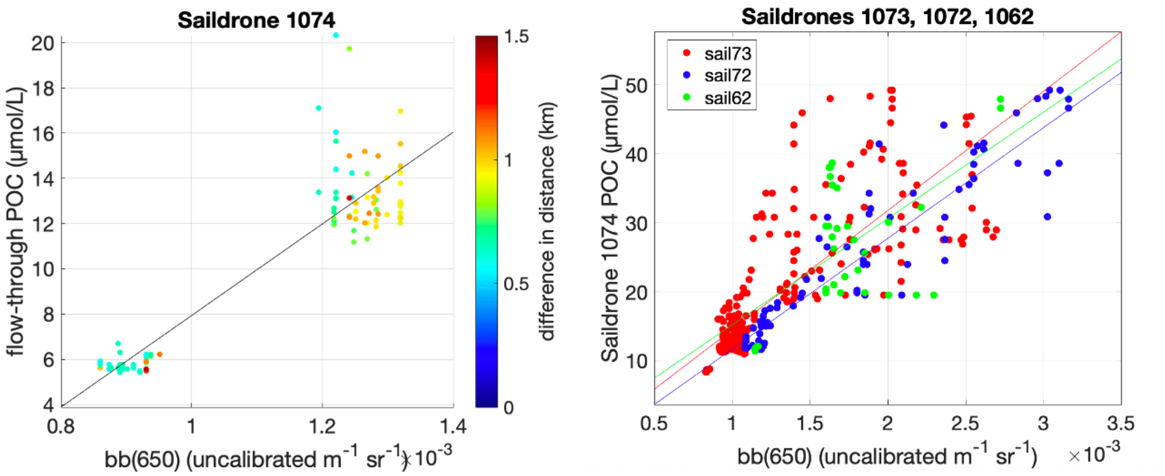

Fig. 26: Left plot: Flow-through POC from cp (y-axis) plotted against Saildrone 1074 bb(650) (x-axis). Points colored by distance between Saildrone and ship. Linear fit in black. Right plot: Calibrated Saildrone 1074 POC (y-axis) plotted against Saildrone 1073 (red), Saildrone 1072 (blue), and Saildrone 1062 (green) bb(650) (x-axis). Linear fits in colors corresponding to Saildrone.

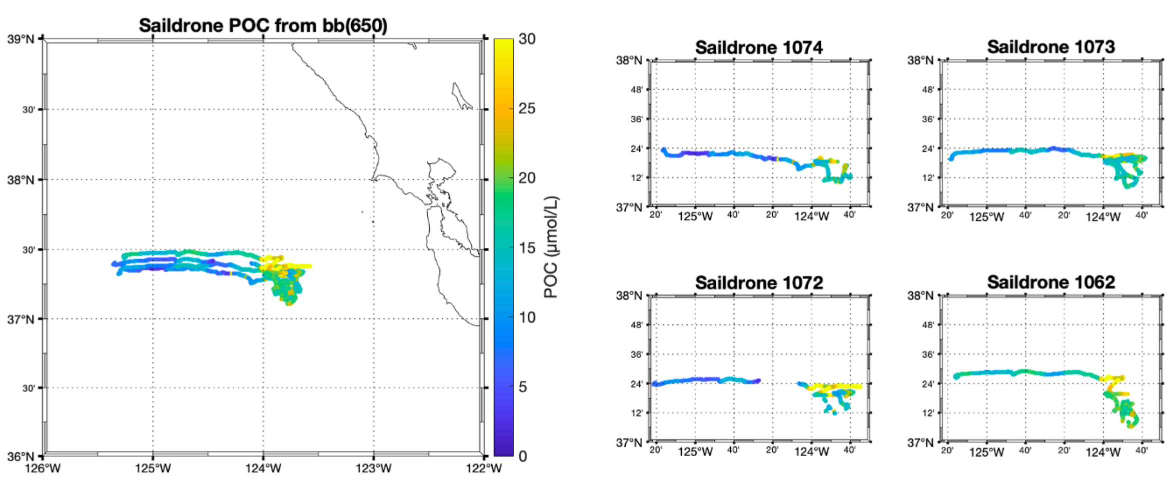

Fig. 27: Saildrone tracks colored by POC (µmol/L).

See Section 4 for equations.

<u>3.3.5 Model evaluation of secondary proxies</u>

We evaluated our intercalibrations with the metrics of root mean square error (RMSE, Eq. 20) and mean absolute percent difference (MAPD, Eq. 21).

$$RMSE = \sqrt{\frac{1}{n}\sum_{i=1}^{n}(x_{model,i} - x_{observed,i})^2} \quad (20)$$

$$MAPD = \frac{1}{n}\sum_{i=1}^{n}\left|\frac{x_{model,i} - x_{observed,i}}{x_{observed,i}}\right| \times 100\% \quad (21)$$

RMSE and MAPD values for all 4 Saildrones were relatively low, indicating that the calibrations were accurate relative to the calibrated reference instrument (Table 1).

Table 1: Model skill metrics for chlorophyll calibrations

Instrument	**RMSE (µg/L)**	**MAPD (%)**
EcoCTD	0.16	22.4
Saildrone 1074	0.06	32.7
Saildrone 1073	0.14	14.2
Saildrone 1072	0.23	20.73
Saildrone 1062	0.22	25.9

Table 2: Model skill metrics for POC calibrations

Instrument	**RMSE (µmol/L)**	**MAPD (%)**
Saildrone 1074	1.64	9.16
Saildrone 1073	5.44	16.21
Saildrone 1072	4.25	12.21
Saildrone 1062	7.67	27.48

4. Summary

Table 3: Summary of underway calibrations

Proxy	**Calibration equation**
Chl-Fl based chlorophyll	[Chl µg/L] = 3.96 [Chl-Fl (µg/L)] – 0.778

cp based chlorophyll	[Chl µg/L] = 3.46[c_p (m^{-1})]$^{3.4}$
POC	[POC µmol/L] = 42.5 [c_p (m^{-1})]$^{3.03}$
PON	[PON µmol/L] = 5.53 [c_p (m^{-1})]$^{2.74}$

Table 4: Summary of EcoCTD calibrations

Proxy	**Calibration equation**
Chl-Fl based chlorophyll	[Chl µg/L] = 1.02 [Chl-Fl (µg/L)] – 0.058
POC	[POC µmol/L] = 8142[bb(700) ($m^{-1}sr^{-1}$)] – 4.85
PON	[PON (µmol/L)] = 994.3 [bb(700) ($m^{-1}sr^{-1}$)] – 3.09

Table 5: Summary of Saildrone calibrations

Platform	**Calibration equations**
Saildrone 1074	[Chl µg/L] = $10^{-0.1550}$ [Chl-Fl (µg/L)] – 0.125 [POC µmol/L] = 20256 [bb(650) ($m^{-1}sr^{-1}$)] – 12.30
Saildrone 1073	[Chl µg/L] = $10^{-0.176}$ [Chl-Fl (µg/L)] – 0.153 [POC µmol/L] = 17278 [bb(650) ($m^{-1}sr^{-1}$)] – 2.75
Saildrone 1072	[Chl µg/L] = $10^{-0.227}$ [Chl-Fl (µg/L)] – 0.0974 [POC µmol/L] = 16054 [bb(650) ($m^{-1}sr^{-1}$)] – 4.35
Saildrone 1062	[Chl µg/L] = $10^{-0.156}$ [Chl-Fl (µg/L)] – 0.238 [POC µmol/L] = 15420 [bb(650) ($m^{-1}sr^{-1}$)] – 0.199

References

Baith, K., Lindsay, R., Fu, G., McClain, C.R., (2001). Data analysis system developed for ocean color satellite sensors. Eos, Transactions American Geophysical Union 82, 202–202. https://doi.org/10.1029/01EO00109

Behrenfeld, & Boss, E. (2006). Beam attenuation and chlorophyll concentration as alternative optical indices of phytoplankton biomass. Journal of Marine Research, 64. https://doi.org/10.1357/002224006778189563

Boss, E., and Pegau, S.W., "Relationship of light scattering at an angle in the backward direction to the backscattering coefficient," Appl. Opt. 40, 5503-5507 (2001)

Farrar, T., et al. (2020), S-MODE: The Sub-Mesoscale Ocean Dynamics Experiment, 3533-3536, doi:10.1109/IGARSS39084.2020.9323112.

Lynn, R. J., S. J. Bograd, T. K. Chereskin, and A. Huyer, Seasonal renewal of the California Current: The spring transition off California, J. Geophys. Res., 108(C8), 3279, doi:10.1029/2003JC001787, 2003.

McDougall, T.J. and P.M. Barker, 2011: Getting started with TEOS-10 and the Gibbs Seawater (GSW) Oceanographic Toolbox, 28pp., SCOR/IAPSO WG127, ISBN 978-0-646-55621-5.

Zhang, X., Hu, L., and He, M.X. (2009), Scattering by pure seawater: Effect of salinity, Optics Express, Vol. 17, No. 7, 5698-5710